Kinematic Optimization of a Spherical Mechanism for a Minimally Invasive Surgical Robot

Mitchell J.H. Lum[1], Jacob Rosen[1,2], Mika N. Sinanan[2,1], Blake Hannaford[1,2]
[1]Department of Electrical Engineering
[2]Department of Surgery
University of Washington
Seattel WA, 98195-2500
E-mail: <mitchlum, rosen, mssurg, blake>@u.washington.edu
URL: http://brl.ee.washington.edu

Abstract— **Advances in surgical technology allow physicians to more effectively provide care to their patients. Minimally invasive surgery (MIS) has revolutionized the way a significant number of procedures are performed. Recent advances in technology have led to the fusion of MIS techniques and robotic devices; however, such systems are currently large and cumbersome. By optimizing a spherical mechanism based on *in-vivo* data collected during MIS procedures, this paper focuses on a bottom-up approach in developing a new class of surgical robot arms. The spherical mechanism is a rotational manipulator with all axes intersecting at the center of the sphere. Locating the rotational center of the mechanism at the MIS port makes this class of mechanism a suitable candidate for the first two links of a surgical robot for both minimally invasive and open surgery. For optimizing the mechanism structure, the forward and inverse kinematics, as well as the Jacobian matrix, were derived. Using the Jacobian, mechanism isotropy was considered as the performance metric. The dexterous workspace (DWS) is defined as a high dexterity region defined by a right circular cone with a vertex angel of 60º in which 95% of the tool motions are contained based on in-vivo measurements. The extended dexterous workspace (EDWS) is defined as the workspace required to reach the entire abdominal cavity with MIS instruments and defined by a cone with an elliptical cross section created by two orthogonal vertex angels of 60º and 90º Optimization across both the DWS and a superset of the EDWS led to a mechanism configuration with link length angles of 74º and 60º that maximizes kinematic performance and compactness. The workspace of this design covers the entire EDWS and is the optimal design for the next generation of surgical manipulator. By directly applying in-vivo experimental data from MIS in order to optimize the spherical manipulator a design that maximizes performance and minimizes size has been developed. A pair of prototype manipulators will be developed based on these results.**

Keywords- Specical Mechanism, Serial Mechanism, Jacobian; Isotropy; Optimization; Minimally Invasive Surgery, Surgical Robot

I. INTRODUCTION

Medicine in general and surgery in particular are subject to profound changes which redefines physicians' capabilities in performing clinical procedures and their abilities to deliver healthcare to local and remote sites. For decades surgery and robotics were progressing in two parallel paths. In surgery, minimally invasive surgery (MIS) revolutionized the way a significant number of surgical interventions are performed. In robotics, teleoperation and computer vision were developed for integrating the human into a robotic system by providing better vision capabilities for the operator. Only in the last decade have surgery and robotics reached a certain maturity that allowed safe assimilation between the two in a teleoperation mode for creating a new kind of operating room accompanied with a long view into the future [1].

As a result of long and extensive research in academia [2-8] and industry, robotic surgery can now be performed. In the United States there are commercially available systems: daVinci by Intuitive Surgical [9-11] and ZEUS by Computer Motion [12,13], which recently merged with Intuitive Surgical. These two systems are currently FDA (Food Drug Administration) approved for specific cardiac and thoracic surgical procedures.

One shortcoming of many of the existing systems is that they are large and cumbersome, occupying large volumes around the operating table and above the patient. These large systems are subject to self-collision and have an added drawback that the large mass and inertia in the surgical arms make incorporating force feedback for enhancing the teleoperation difficult. Using an optimized spherical mechanism architecture based on extensive database of force/torque position/orientation of surgical tools acquired in-vivo during minimally invasive surgery [14,15] may provide a solid foundation for a bottom-up approach in developing a new class of surgical arms.

Generic spherical mechanisms were subjects of previous research both in their serial and parallel configurations [16-18]. However the generic optimization criteria used for optimizing their structure did not match the special workspace associated with surgery. In the current study, the structure of a serial spherical mechanism was optimized for operating in a well-defined workspace. The definition of the workspace was based on an extensive in-vivo measurements obtained during minimally invasive surgery [14,15].

Research Sponsored by U.S. Army. DAMD17-02-1-0202 "MiniRobot Design for Military Telesurgery in the Battlefield: Breaking the size barrier for surgical manipulators" exact grant need title and number

II. MANIPULATOR KINEMATICS

A. Spherical Mechanism - Conventions and Notation

The mechanism under study is member of a class of spherical mechanism in which all the links' rotation axes intersect at a single point located at the center of the mechanism. Aligning this point with the location of the port through which tools are inserted into the body in MIS eliminates any tool translation along the orthogonal axes of the tool's shaft that are inherently imposed by the presence of the port. The center of the sphere is the origin for all reference frames of the mechanism. Thus, each frame is a pure rotation from one to the next.

The frames are assigned such that the Z-axis of the n^{th} frame points outward along the n^{th} joint [19]. The numbering scheme for the frames has odd numbers (Frames 0', 1, 3 and 5). The fixed, end-effector, frame is Frame 5. Frame 0' is oriented such that the z-axis points along joint 1 and the y-axis points to the apex of the sphere. The link angle, α_{i+1} expresses the angle between the ith and $(i+1)$th axis. These are fixed parameters defined by the mechanism geometry. The rotation angle θ_i defines the angle between the rotation axis i-1 and i. When all joint angles are set to 0 ($\theta_1=\theta_3=0$), link α_{13} lies in a plane defined by $Z_{0'}$ and $Y_{0'}$, link α_{35} is folded back on link α_{13}.

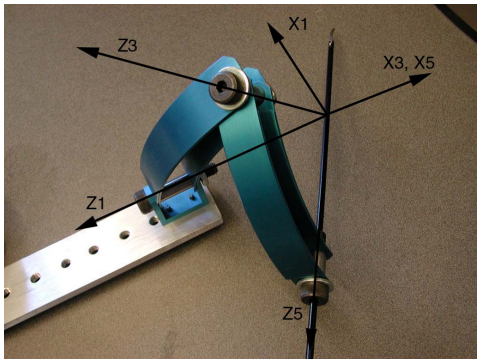

Figure 1. Spherical serial two link mechanism with corrdinate assigment

The transformation matrices between frames are based on the Denavit-Hartenberg (DH) parameter notation and summarized in Table I. Since no translations exist between the assigned coordinate systems the transformation matrix is reduced from the typical 4x4 matrix, to a 3x3 rotation matrix.

TABLE I. SERIAL MANIPULATOR D-H PARAMETERS

i-1	i	$i+1$	α_{i-1}	θ_i
0'	1	3	0	θ_1
1	3	5	$-\alpha_{13}$	θ_3
3	5	-	α_{35}	$-\theta_5 = 0$

B. Forward Kinematics

Given the mechanism parameters (α_{i-1}, θ_i) the forward kinematics express the orientation of the end-effector ${}^{0'}u$ in Frame 0'.Using the DH notation along with the DH parameters defined in Table I the generalized rotation matrix is defined as follows:

$$ {}^{i-1}_{i}R = \begin{bmatrix} \cos\theta_i & -\sin\theta_i & 0 \\ \sin\theta_i * \cos\alpha_{i-1} & \cos\theta_i * \cos\alpha_{i-1} & -\sin\alpha_{i-1} \\ \sin\theta_i * \sin\alpha_{i-1} & \cos\theta_i * \sin\alpha_{i-1} & \cos\alpha_{i-1} \end{bmatrix} \quad (1) $$

The forward kinematics from the base, Frame 0' to the end effector, Frame 5 is the product of those rotation matrices.

$$ {}^{0'}_{5}R = {}^{0'}_{1}R * {}^{1}_{3}R * {}^{3}_{5}R \quad (2) $$

Rather than expressing the entire end-effector frame, it is sensible to express a vector that represents the axis along which the surgical tool will point. Tool roll, θ_5, is not represented, as it will be designed onto the distal end of the mechanism later. Let ${}^{0'}u$ be a vector pointing along the end-effector axis, z_5 expressed in Frame 0'.

$$ {}^{0'}u = {}^{0'}_{5}R * \begin{bmatrix} 0 \\ 0 \\ 1 \end{bmatrix} = \begin{bmatrix} {}^{0'}u_x \\ {}^{0'}u_y \\ {}^{0'}u_z \end{bmatrix} = \quad (3) $$

$$ \begin{bmatrix} \cos\theta_1 * \sin\theta_3 * \sin\alpha_{35} + \sin\theta_1 * \cos\theta_3 * \cos\alpha_{13} * \sin\alpha_{35} - \sin\theta_1 * \sin\alpha_{13} * \cos\alpha_{35} \\ \sin\theta_1 * \sin\theta_3 * \sin\alpha_{35} - \cos\theta_1 * \cos\theta_3 * \cos\alpha_{13} * \sin\alpha_{35} - \cos\theta_1 * \sin\alpha_{13} * \cos\alpha_{35} \\ \cos\theta_3 * \sin\alpha_{13} * \sin\alpha_{35} + \cos\alpha_{13} * \cos\alpha_{35} \end{bmatrix} $$

C. Inverse Kinematics

From the vector ${}^{0'}u$ that expresses the z-axis of the end-effector and the mechanism parameters (α_{i-1}) the inverse kinematics aim to express the mechanism joint angles θ_i. Using the expression for ${}^{0'}u_z$ (the third line of ${}^{0'}$u –Eq. 3) and solving for $\cos\theta_3$ results in

$$ \cos\theta_3 = \frac{{}^{0'}u_z - \cos\alpha_{13} * \cos\alpha_{35}}{\sin\alpha_{13} * \sin\alpha_{35}} \quad (4) $$

Given an expression for cosine of θ_3 there are two possible solutions for θ_3, one corresponding to an elbow up and one for the elbow down configuration. The two solutions for θ_3 are as follows:

$$ \theta_{3a}, \theta_{3b} = a\tan 2\left(\pm\sqrt{1-\cos^2\theta_3}, \cos\theta_3 \right) \quad (5) $$

Using the expression for ${}^{0'}u_x$ and ${}^{0'}u_y$ (the first and second lines of ${}^{0'}$u –Eq. 3) then solving for $\sin\theta_1$ and $\cos\theta_1$ and finally θ_1 results in Eq 6.

$$\cos\theta_1 = \frac{{}^{0'}u_x * \sin\theta_3 * \sin\alpha_{35} - {}^{0'}u_y * (\cos\theta_3 * \cos\alpha_{13} * \sin\alpha_{35} - \sin\alpha_{13} * \cos\alpha_{35})}{(\sin\theta_3 * \sin\alpha_{35})^2 + (\cos\theta_3 * \cos\alpha_{13} * \sin\alpha_{35} - \sin\alpha_{13} * \cos\alpha_{35})^2}$$
$$\sin\theta_1 = \frac{{}^{0'}u_y * \sin\theta_3 * \sin\alpha_{35} + {}^{0'}u_x * (\cos\theta_3 * \cos\alpha_{13} * \sin\alpha_{35} - \sin\alpha_{13} * \cos\alpha_{35})}{(\sin\theta_3 * \sin\alpha_{35})^2 + (\cos\theta_3 * \cos\alpha_{13} * \sin\alpha_{35} - \sin\alpha_{13} * \cos\alpha_{35})^2} \quad (6)$$
$$\theta_1 = a\tan 2(\sin\theta_1, \cos\theta_1)$$

Once the values for θ_3 corresponding to elbow up/down configurations are solved, the associated values for θ_1 can be solved using Eq. 6. Thus the inverse kinematic equations provide two solutions to the pose of the manipulator, θ_{1a} and θ_{3a}, and θ_{1b} and θ_{3b}.

D. Jacobian Matrix

The Jacobian matrix relates joint velocities to end-effector angular velocities. It can be expressed with respect to any of the frames associated with the mechanism. If the Jacobian is expressed in Frame 5, the eigenvalue corresponding to the angular velocity of Frame 5 has a value of 1 for all poses and joint velocities. The mechanism under analysis is viewed as a 2 DOF manipulator, thus the upper 2x2 submatrix of the full 3x3 Jacobian relates the two controlled joint velocities, 1 and 3 to end- effector velocity.

In the most general sense a recursive expression of the angular velocity is expressed in Eq. 7 [19]

$$\left[{}^{i+1}\omega_{i+1}\right] = \left[{}^{i+1}_{i}R\right]\left[{}^{i}\omega_{i}\right] + \dot{\theta}^{i+1}_{i+1}\,\hat{z}_{i+1} \quad (7)$$

By distributing and rearranging, the expression from the end effector frame, Frame 5, to the base frame, Frame 0' is stated as

$$\left[{}^{5}\omega_{5}\right] = \left[{}^{5}_{1}R\right]\begin{bmatrix}0\\0\\1\end{bmatrix}\dot{\theta}_1 + \left[{}^{5}_{3}R\right]\begin{bmatrix}0\\0\\1\end{bmatrix}\dot{\theta}_3 + \begin{bmatrix}0\\0\\1\end{bmatrix}\dot{\theta}_5 \quad (8)$$

which is combined into:

$$\begin{bmatrix}{}^{5}\omega_{5x}\\ {}^{5}\omega_{5y}\\ {}^{5}\omega_{5z}\end{bmatrix} = \left[\left[{}^{5}_{1}R\right]\begin{bmatrix}0\\0\\1\end{bmatrix} \quad \left[{}^{5}_{3}R\right]\begin{bmatrix}0\\0\\1\end{bmatrix} \quad \begin{bmatrix}0\\0\\1\end{bmatrix}\right]\begin{bmatrix}\dot{\theta}_1\\ \dot{\theta}_3\\ \dot{\theta}_5\end{bmatrix} \quad (9)$$

Based on the previous justification, the upper 2x2 submatrix of the full 3x3 Jacobian is taken to yield a truncated 2x2 version relating the controlled axes of motion to the end effector velocity and is expressed in Eq. 10

$$\begin{bmatrix}{}^{5}\omega_{5x}\\ {}^{5}\omega_{5xy}\end{bmatrix} = \left[J_{5\,truncated}\right]_{2x2}\begin{bmatrix}\dot{\theta}_1\\ \dot{\theta}_3\end{bmatrix} \quad (10)$$

This version of the Jacobian is further used for calculating the manipulator isotropy.

III. Mechanism Optimization

A. Workspace Requirments for Minmally Invasive Surgical Robot and Practical Joint Limits

The Blue DRAGON is a system for measuring the position and orientation of two endoscopic tools along with the forces and torques applied to the tools in a minimally invasive environment [14]. Analyzing a database of generic surgical tasks including tissue handling/examination, tissue dissection, and suturing performed on an animal model in-vivo by 30 surgeons in a MIS environment indicates that 95% of the time the surgical tools positions encompass a 60º cone with a tip located at the port. In addition, measuring the reachable workspace of an endoscopic tool performed on a human model shows that in order to reach the full extent of the abdomen the tool needed to be moved 90º in the lateral/medial direction (left to right) and 60º in the superior/inferior (foot to head) direction.

The reachable workspace of the spherical manipulator is a sector of a sphere. The size and the shape of this sector are determined by the mechanism joint lengths (α_{13}, α_{35}), joint angles (θ_1, θ_3) and the radius of the sphere. Based on the in-vivo measurements, the dexterous workspace (DWS) for the surgical robot was defined as the area on the sphere bounded by the closed line created when a right circular cone with a circular cross section and a vertex angle of 60º located at the center of the sphere intersected the sphere. The extended dexterous workspace (EDWS) of the surgical robot is defined in a similar fashion; however, the cone has an elliptical cross section created by two orthogonal vertex angels of 60º and 90º. The optimizing process aimed to define the mechanism parameters (link length) allowing it to reach the EDWS and provide high dexterity in the DWS.

An acceptable compromise between the general requirement to design a small form factor mechanism with a limited high dexterity workspace and yet creating it big enough allowing it to reach the extended workspace as required in surgery was achieved by optimizing the mechanism link lengths to allow maximal dexterity in the DWS while including the EDWS in its reachable workspace.

Up to this point, the analysis has been purely mathematical. The manipulator could move through singularities, fold on itself and solve for arbitrary poses without regard to how a physical device might accomplish this. Based on the mechanical design of the mechanism, the range of motion of the first joint angle is 180º ($0º<\theta_1<180º$) and the range of motion of the second angle is 160º ($20º<\theta_3<180º$). These constraints limit the design space from which an optimal solution was sought.

B. Mechanism Isotropy

The Jacobian matrix allows one to analyze the kinematic performance of a mechanism. A common performance metric is mechanism manipulability [20]. This analysis uses mechanism isotropy as the performance metric. Isotropy is defined in Eq. 11 as the ratio between the lowest eigenvalue and the highest eigenvalue of the Jacobian.

$$ISO(\theta_1,\theta_3)=\frac{\lambda_{\min}}{\lambda_{\max}} \qquad ISO\in\langle 0,1\rangle \tag{11}$$

Given a design candidate (a pair of link angles α_{13} and α_{35}), for every given mechanism pose the associated isotropy value is in the range of 0 to 1. An isotropy measure of 0 means the mechanism is in a singular configuration and has lost a degree of freedom; in other words, there is a direction in which it can no longer move. A measure of 1 means that the eigenvalues of the Jacobian are all equal and the mechanism can move equally well in all directions.

C. Scoring Criteria

Each design candidate (a pair of link angles α_{13} and α_{35}) must be assigned a single score so the best overall manipulator design can be selected. Three individual criteria including: (1) an integrated average score, (2) a minimal single score, (3) the cube of the angular length of the links are incorporated into the composite score and expressed in Eq.12.

Mechanism isotropy is a performance measure for a particular pose of the manipulator. In order to analyze the mechanism a hemisphere is discretized into points distributed equally in azimuth and elevation. The distribution of points in equal azimuth and elevation causes each point to be associated with a different area based on elevation. One measure of how well a manipulator performs is to calculate the isotropy at each point, multiply by its corresponding surface area then sum all of the weighed point-scores over the sector generated when a cone with head angle of 60º and located at the center of the sphere intersects the reachable part of the hemisphere given the mechanism joint constrains previously defined. This score provides an average performance over the entire section intersected by the cone.

Given the ranges of the azimuth angle σ and the elevation angle ζ, defining the intersection area between a right circular cross section cone with a vertex angel of 60º located at the center of the sphere and the sphere itself, the set, K, of all possible intersection areas on the hemisphere is

$$K=\{k(\sigma,\zeta):0<\sigma<2*\pi,0<\zeta<\pi/4\}$$

The set of all the discrete points contained in the intersection area is

$$k^p_{\sigma,\zeta}\subset k_{\sigma,\zeta}$$

Due to the discrete nature of the computation, each point included in the intersection area has an associated isotropy value *ISO* and sector area *A*. Thus the overall scoring functions are

$$S_{sum}=\underset{K}{MAX}\left\{\sum_{k^p_{\sigma,\zeta}} ISO(\theta_1,\theta_3)*A(\sigma,\zeta)\right\} \tag{12a}$$

$$S_{\min}=\underset{K}{MAX}\left\{\underset{k^p_{\sigma,\zeta}}{MIN}(ISO(\theta_1,\theta_3))\right\} \tag{12b}$$

There are many orientations of the DWS with respect to the hemisphere, noted as the set *K*. Each element of *K* has a different summed isotropy. The value, S_{sum}, is the largest of the summed isotropy scores. In other words, each design candidate has an S_{sum} value that corresponds to the highest summed isotropy score for that design.

The limitation of a summed isotropy score is that singularities or workspace boundaries could exist within a region that has a good score. The minimum isotropy value within the cone intersection area is an indicator of the worst performance that can be expected over that cone intersection area. Each element in K has a different minimum isotropy value. S_{min} is the highest minimum isotropy score on the set of all cones, K. In other words, each design candidate has a S_{min} value that corresponds to the highest minimum isotropy score for that design.

A design with greater link angles will have a larger reachable workspace and generally better S_{sum} and S_{min} values. The drawback to larger link angles is a decrease in link stiffness. As suggested by the experimental findings, in surgery the mechanism needs to be operated in a limited workspace. The goal would be to maximize the kinematic performance over the surgical workspace while minimizing the link length. Static analysis of a cantilever beam shows that the arm stiffness is inversely proportional to the cube of length.

The overall score takes in to account all three individual criteria is defines as follows

$$\phi=\frac{S_{\text{sum}}\cdot S_{\min}}{(\alpha_{13}+\alpha_{35})^3} \tag{13}$$

A requirement of the optimization is that over the 60º-cone, the mechanism does not encounter any singularities or workspace boundaries. Multiplying the summed isotropy with the minimum isotropy, candidates that fail to meet the requirement have a score of zero. Dividing by the cube of the sum of the link angles the score reflects proportionality to the mechanisms stiffness. Thus, over a scan of the potential design space, the peak composite score represents a design with maximum average performance, a guaranteed minimum performance and maximized stiffness.

D. Optimization Algorithm

The optimization considered all combinations of α_{13} and α_{35} from 16º to 90º in 2º increments for a total of 1444 design candidates considered. The hemisphere was discretized into 3600 points, distributed evenly in azimuth and elevation.

$$min\ \phi(\alpha_{13},\alpha_{35},\theta_1,\theta_3)\quad\begin{cases}16^o<\alpha_{13}<90^o\\16^o<\alpha_{35}<90^o\\\theta_1\in DWS\\\theta_3\in DWS\end{cases} \tag{14}$$

Considering the DWS, its orientation in azimuth and elevation are varied in order to obtain the best cone for that design candidate. However, optimizing the EDWS, which is an elliptical cone, would add another design parameter, namely cone roll angle. Introducing an additional parameter will increase execution time of the optimization by an order of magnitude. By utilizing a 90º cone that encompasses the EDWS the additional design parameter is avoided. However, this could force the link lengths to be larger than necessary.

For example a design that can reach 60º in one direction and 90º in an orthogonal direction may satisfy the EDWS cone but not a 90º cone.

IV. Results

Using the definition of the scoring criteria and hemisphere point resolution of 2º, a numerical scan of the design space was performed using all the combinations of link angles α_{13} and α_{35} in the range of 16º to 90º. For the serial manipulator, optimizing on the DWS, the best design was achieved with link angles of α_{13}=52º and α_{35}=40º and a score of 0.0520 (Fig. 2a). In contrast, running same optimization but requiring a 90º cone indicated that the optimal mechanism design has link angles α_{13}=90º and α_{35}=72º with a score of 0.0471 (Fig. 2b).

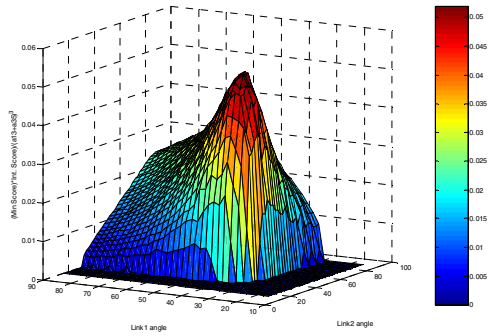

(a)

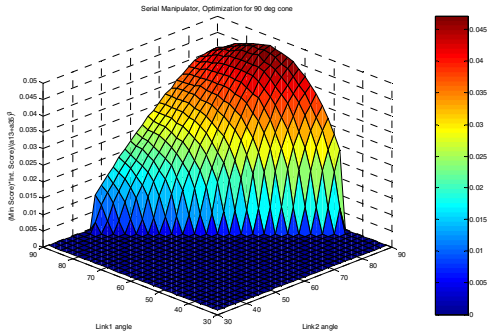

(b)

Figure 2. Serial Manipulator, Design Space Optimization for the (a) DWS, 60 degree cone (b) 90 degree cone

The difference in the results is not unexpected but it does pose an interesting dilemma. If one chooses the design that optimizes on a 90º cone, the resulting design should be more likely to reach all the poses that manipulator would be asked to reach. However, this design has lower overall performance than the design optimized on for the DWS and larger links, which may increase the likelihood for problems of collisions between two manipulators.

One interesting consideration is to take the best design that is optimized for the DWS that also has the ability to reach a 90º cone. This is done by taking the set of designs from the 90º cone optimization with a non-zero score (these are all designs which have some 90º cone that contains no singularities) and run an optimization on this subset of designs. Effectively it takes the DWS optimization and slices out the designs that cannot reach a 90º cone.

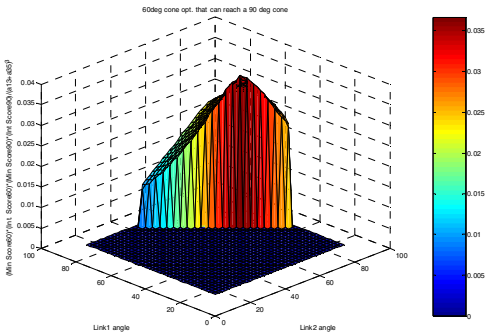

Figure 3. Design Space Optimization of 60 degree cone that can reach 90 degree cone

The resulting peak in the design space is α_{13}=74º and α_{35}=60º with a score of 0.0367. This design is a compromise of the DWS optimization and the 90º-cone optimization.

However as discussed earlier, optimization on a 90º cone may result in a design that is larger than needed. Figure 4 shows that the workspace of the optimal design for the DWS (α_{13}=52º and α_{35}=40º) is a slice of the sphere.

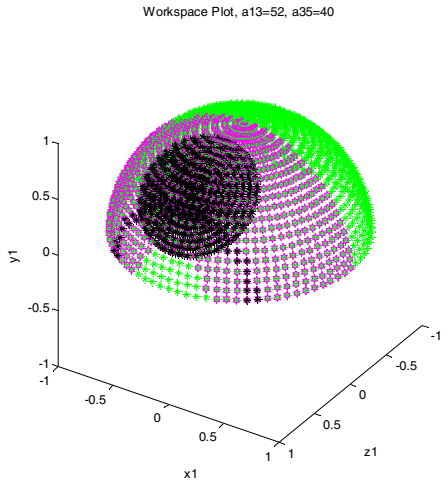

Figure 4. Workspace plot for α_{13}=52º and α_{35}=40º. This workspace plot shows the hemisphere in green, the reachable workspace in purple, and the orientation of the best 60º cone in black, with the strip of maximum isotropy also in black.

V. Discussion

This paper has shown the development of the kinematic equations for the serial spherical manipulator with link angles less than 90º. Optimization of the mechanism specifically for surgery yields a more compact device than a general spherical manipulator. The optimization balanced between a guaranteed minimum and integrated isotropy over the DWS as well as total

link length in order to yield a very compact, highly dexterous mechanism.

While the results yield a compact high performance manipulator, dynamic performance was not considered. A more complete optimization could include placement of two manipulators over a patient and would include parameters such as robot-patient collisions as well as robot-robot collisions and self-collision.

Directly applying the Blue DRAGON experiments to the robot design must be done with some caution. Although the animal models are similar in anatomy to humans, the results may not be directly applicable in human surgical procedures.

REFERENCES

[1] Satava, R. Disruptive visions: the operating room of the future, Surgical Endoscopy, 2003, *17*(1), 104-107.

[2] Hannaford, B. Feeling is Believing: Haptics and Telerobotics Technology. In The Robot in the Garden, Telerobotics and Telepistomology on the Internet, Cambridge, MA, 1999; Goldberg, J.K.; MIT Press: Cambridge, MA, 1999.

[3] Taylor, R.; Lavallee, S.; Burdea, G.; Mosges, R. Computer-Integrated Surgery, MIT Press: Cambridge, MA, 1996.

[4] Howe, R.; Matsuoka, Y. Robotics for Surgery. In *Annual Review of Biomedical Engineering*, 1999, *1*, 211 - 240.

[5] Buess, G.; Schurr, M.; Fischer; Sabine C. Robotics and Allied Technologies in Endoscopic Surgery. Archives of Surgery, 2000, *135*, 229-235.

[6] Cleary, K.; Nguyen, C. State of the Art in Surgical Robotics: Clinical Applications and Technology Challenges. In *Computer Aided Surgery*, 2001, *6*, 312-328.

[7] Ballantyne G. Special Issue on Surgical Robotics, Surgical Laparoscopy, Endoscopy & Percutaneous Techniques, 2002, *12*(1).

[8] Speich J.E. and J.Rosen, Medical Robotics, Encylopedia of Biomedical Engineering, Add editor, To be pulished in 2004

[9] http://www.intuitivesurgical.com/.

[10] Guthart, G.; and Salisbury, K. The Intuitive™ Telesurgery System: Overview and Application, Proceedings of 2000 IEEE International Conference on Robotics and Automation, 618-621, 2000.

[11] Madhani, A.; Niemeyer, G.; Salisbury, K. The Black Falcon: A Teleoperated Surgical Instrument for Minimally Invasive Surgery. *IEEE/RSJ Int.* Conf. on Intelligent Robots and Systems (IROS), Victoria B.C., Canada, October, 1998.

[12] http://www.computermotion.com/.

[13] Marescaux, J.; Leroy, J.; Gagner, M.; Rubino, F.; Mutter, D.; Vix, M.; Butner, S.; Smith, M.K. Transatlantic Robot-Assisted Telesurgery, Nature Magazine, 2001, 413, 379-380.

[14] Rosen, J.; Brown, J.; Chang, L.; Barreca, M.; Sinanan, M.; Hannaford, B. The Blue DRAGON - A System for Measuring the Kinematics and the Dynamics of Minimally Invasive Surgical Tools In–Vivo, Proceedings of the 2002 IEEE International Conference on Robotics & Automation, Washington DC, USA, May 11-15, 2002.

[15] J.D. Brown. "***In-Vivo*** and Postmortem Biomechanics of Abdominal Organs Under Compressive Loads: Experimental Approach in a Laparoscopic Surgery Setup." University of Washington, PhD. Dissertation, August, 2003.

[16] M. Ouerfelli, V. Kumar. "Optimization of a Spherical Five-Bar Parallel Drive Linkage". Transactions of the ASME vol. 116: pp. 166-173, 1994.

[17] Kurtz and Hayward. "Multiple-Goal Kinematic Optimization of a Parallel Spherical Mechanism with Actuator Redundancy," IEEE 1992.

[18] Jean-Pierre Merlet. "Parallel Robots" Kluwer Academic Publishers, 2000.

[19] Craig. "Introduction to Robotics," 2nd ed. Addison Wesley, 1989.

[20] Yoshikawa, Tsueno. "Manipulability and Redundancy Control of Robotic Mechanisms". IEEE 1985